

Received December 6, 2020, accepted December 25, 2020, date of publication January 11, 2021, date of current version January 26, 2021.

Digital Object Identifier 10.1109/ACCESS.2021.3050749

Research on Evaluation Method of Time Transfer Performance Between Ground Stations in Two-Way Satellite Comparison Network

WEI WANG^{1,2,3}, XUHAI YANG^{1,2,3}, WEICHAO LI^{1,3}, YULONG GE^{1,2,3}, LIANG CHEN^{1,3}, FEN CAO^{1,3}, PEI WEI^{1,2,3}, PENG LIU⁴, AND ZHIGANG LI^{1,3}

¹National Time Service Center, Chinese Academy of Sciences, Xi'an 710600, China

²School of Astronomy and Space Science, University of Chinese Academy of Science, Beijing 100049, China

³Key Laboratory of Precision Positioning and Timing Technology, National Time Service Center, Chinese Academy of Sciences, Xi'an 710600, China

⁴39th Research Institute, China Electronics Technology Group Corporation, Xi'an 710600, China

Corresponding author: Xuhai Yang (yyang@ntsc.ac.cn)

This work was supported in part by the CAS "Light of West China" Program under Grant XAB2018YDYL01 and in part by the National Natural Science Foundation of China under Grant 12073034.

ABSTRACT High-precision time synchronization between ground stations is essential for the precise measurement and determination of satellite orbits. Among the numerous time synchronization methods available, two-way satellite time and frequency transfer (TWSTFT) technology is widely used because of the approximate symmetry of its signal transmission path, such that most of the error terms can be offset to obtain subnanosecond time transmission accuracy. A C-band two-way satellite comparison network has been constructed at National Time Service Center (NTSC), Chinese Academy of Sciences for orbit determination and to compare the times between ground stations. The gradual increase in the number of ground stations has created a problem in need of urgent resolution: the facile and rapid evaluation of the time transfer performance between ground stations by a two-way satellite comparison network without the use of additional equipment. We solve this problem by applying the TWSTFT triangle closure method and the precise point positioning time transfer method to the NTSC two-way satellite comparison network and conduct joint observations between terrestrial stations to evaluate the network time transfer performance. We select the Xi'an, Kashi and Sanya stations of the NTSC two-way satellite comparison network to carry out verification tests. The results show that the NTSC two-way satellite comparison network can achieve subnanosecond time synchronization accuracy. The accuracy of time synchronization between stations can be checked conveniently and quickly without the use of additional equipment. This study presents the most recent developments for the NTSC two-way satellite comparison network and serves as a reference for evaluating the time transfer performance of similar networks.

INDEX TERMS Equipment delay, PPP, triangular closure difference, TWSTFT.

I. INTRODUCTION

Two-way satellite time and frequency transfer (TWSTFT) and precise point positioning (PPP) are the two most accurate remote time transfer technologies available and can reach subnanosecond remote time synchronization accuracy [1]–[5]. Most errors in the signal transmission process are canceled out because of the approximate symmetry of the signal transmission path of TWSTFT technology. The high precision of this technology results from this symmetry [6], [7]. The high precision of PPP technology derives from the

use of observed data from the carrier phase [5], [8], [9]. These two technologies are currently officially employed by Bureau International des Poids et Mesures for international atomic time (TAI) and coordinated universal time (UTC) computation [10]–[12].

National Time Service Center (NTSC), Chinese Academy of Sciences has used TWSTFT technology to establish a two-way satellite comparison network and proposed two-way tracking technology for the high-precision orbit determination of geostationary orbit (GEO) satellites [13]–[15]. High-precision time synchronization between ground stations is essential for high-precision satellite orbit measurement and determination. The objective of this study is to

The associate editor coordinating the review of this manuscript and approving it for publication was Shiwei Xia¹.

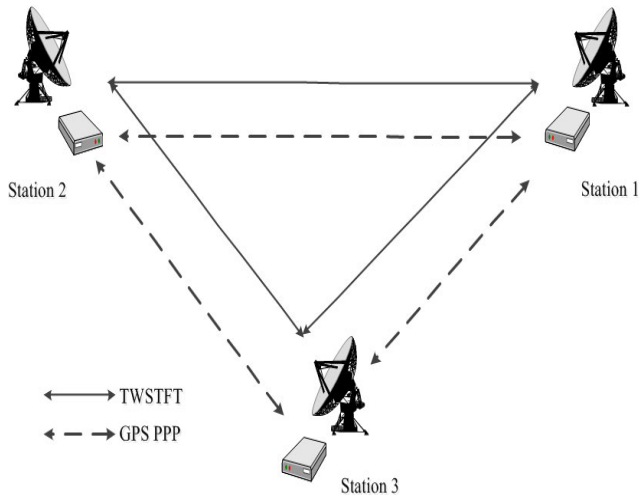


FIGURE 1. Schematic diagram of the evaluation method of time transfer performance between ground stations.

determine how the TWSTFT network can easily and quickly evaluate the accuracy of time synchronization between various stations without the use of additional equipment as the number of ground stations continues to gradually increase.

The international time keeping laboratory calculates the TAI using a multilateral system, for which the working mode is presented in [1]. A model for the comparison links between various laboratories is established, whereby the redundant links generated during the regular time comparison are used to effectively improve the stability of the time comparison for the system. The use of redundant links in the two-way (TW) network for accurate time transfer is also described in [16]. Inspired by the method presented in [1] and [16], we apply the TWSTFT triangular closure method to the NTSC two-way satellite comparison network and carry out joint observations between terrestrial stations to evaluate the time transfer performance [17]–[21]. We further compare the accuracy of TWSTFT between ground stations by carrying out a PPP time transfer experiment simultaneously with the TWSTFT triangle closure experiment. We use the time transfer difference between TWSTFT and PPP to verify the accuracy of time synchronization between ground stations [22], [23]. A schematic of the performance evaluation method is shown in Fig. 1.

II. PRINCIPLE OF TWSTFT

The principle of TWSTFT is illustrated in Fig. 2. Consider two participating ground stations, 1 and 2. At a particular moment within the same timing system, station 1 converts a time signal from a local atomic clock through pseudorandom code modulation with a modem and sends the signal through an antenna to a GEO satellite, which subsequently forwards the signal to station 2. The signal is demodulated and compared with the signal from a local atomic clock to measure the time delay of the signal transmission from station 1 to the satellite to station 2. Station 2 simultaneously and similarly sends a signal to station 1 through the GEO satellite. The data

collected between two ground stations is exchanged to obtain a highly accurate clock difference between the two atomic clocks [24].

One can readily derive the following equations for the time of the signal transmissions in both directions between stations 1 and 2 through a satellite, recorded as time interval counter (TIC) readings:

$$TI(1) = TS(2) - TS(2) + TX(2) + SPU(2) + SCU(2) + SPT(2) + SPD(1) + SCD(1) + RX(1) \quad (1)$$

$$TI(2) = TS(2) - TS(1) + TX(1) + SPU(1) + SCU(1) + SPT(1) + SPD(2) + SCD(2) + RX(2) \quad (2)$$

After subtraction of (2) from (1), the results are as follows in (3):

$$TS(1) - TS(2) = \frac{1}{2} \times \left\{ \begin{array}{l} [TI(1) - TI(2)] + [SPT(1) - SPT(2)] \\ + [TX(1) - RX(1)] - [TX(2) - RX(2)] \\ + [SPU(1) - SPD(1)] \\ - [SPU(2) - SPD(2)] \\ + [SCU(1) - SCD(1)] \\ - [SCU(2) - SCD(2)] \end{array} \right\} \quad (3)$$

where TS(1) and TS(2) represent the local time-scale for station 1 and 2 respectively, TI(1) and TI(2) are the readings of time interval counters for stations 1 and 2, respectively. (The counter gate is turned on by a one-pulse-per-second (1PPS) signal related to the local transmit signal and closed by a 1PPS signal related to the received signal). SPT(1) and SPT(2) are the satellite path delay through the transponder for 1 to 2 communication link and 2 to 1 communication link, respectively; TX(1) and TX(2) are the transmitter delay (including the modem delay) of ground equipments at stations 1 and 2, respectively; RX(1) and RX(2) are the receiver delay (including the modem delay) of ground equipments at stations 1 and 2, respectively; SCU(1) and SCU(2) are the Sagnac correction in the uplink of the stations 1 and 2, respectively; SCD(1) and SCD(2) are the Sagnac correction in the downlink of the stations 1 and 2, respectively; SPU(1) and SPU(2) are the uplink geometric delay of the stations 1 and 2, respectively; SPD(1) and SPD(1) are the downlink geometric delay of the stations 1 and 2, respectively. Equation (3) was from a reference published by the International Telecommunication Union [23]. The items on the right side of (3) have been discussed in many works [15], [25], [26], and are applicable to all types of satellites.

Equation (1) shows the sum SP(2) of the uplink delay SPU(2) of the signal transmitted by the ground station 2, the satellite path delay SPT(2) through the transponder, and the downlink delay SPD(1). This sum represents the total link delay of the signal sent from ground station 2 to the satellite to ground station 1. Equation (1) is given as follows:

$$TI(1) = TS(1) - TS(2) + TX(2) + SP(2) + RX(1) + [SCD(1) - SCD(2)] \quad (4)$$

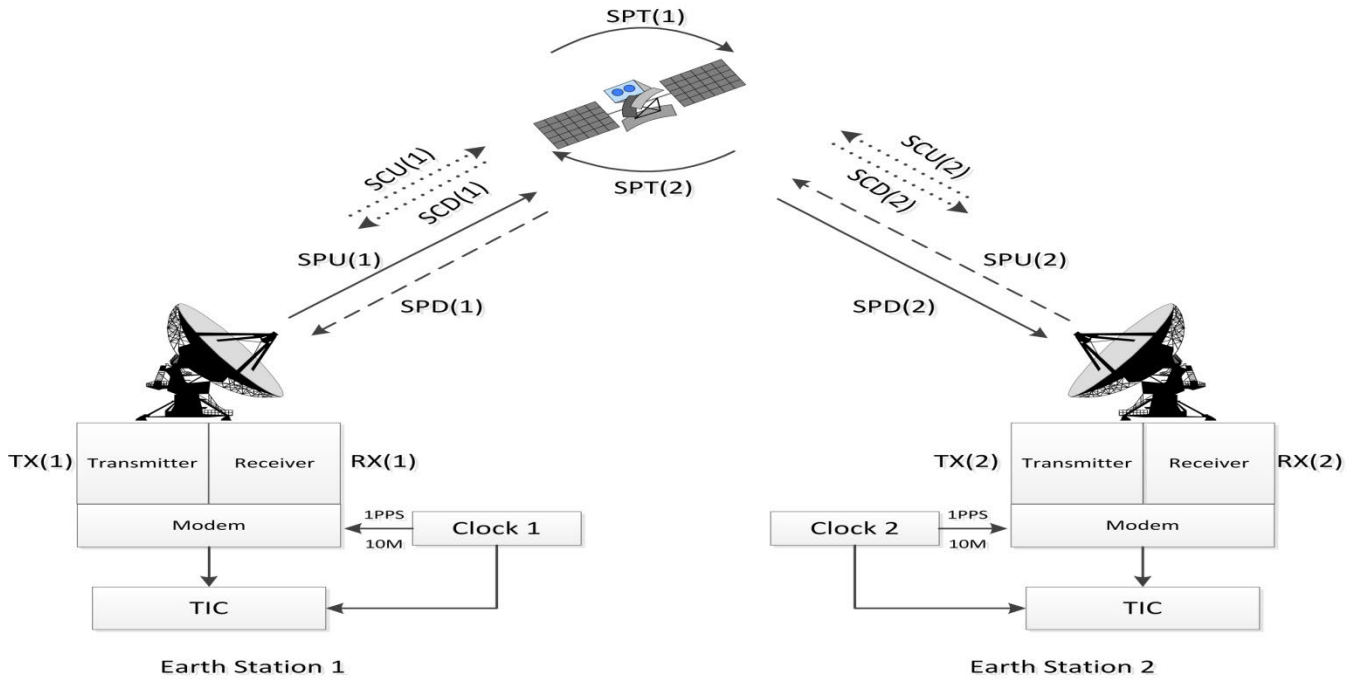


FIGURE 2. Schematic diagram of a TWSTFT system.

Similarly, equation (2) is organized as follows:

$$TI(2) = TS(2) - TS(1) + TX(1) + SP(1) + RX(2) + [SCD(2) - SCD(1)] \quad (5)$$

According to (3), (4) and (5), the clock differences between the three ground stations can be obtained as follows:

$$\begin{aligned} TW(1, 2) &= TS(1) - TS(2) \\ &= 1/2[TI(1) - TI(2)] + 1/2[TX(1) - RX(1)] \\ &\quad - 1/2[TX(2) - RX(2)] + 1/2[SP(1) - SP(2)] \\ &\quad - [SCD(1) - SCD(2)] \end{aligned} \quad (6)$$

$$\begin{aligned} TW(1, 3) &= TS(1) - TS(3) \\ &= 1/2[TI(1) - TI(3)] + 1/2[TX(1) - RX(1)] \\ &\quad - 1/2[TX(3) - RX(3)] + 1/2[SP(1) - SP(3)] \\ &\quad - [SCD(1) - SCD(3)] \end{aligned} \quad (7)$$

$$\begin{aligned} TW(2, 3) &= TS(2) - TS(3) \\ &= 1/2[TI(2) - TI(3)] + 1/2[TX(2) - RX(2)] \\ &\quad - 1/2[TX(3) - RX(3)] + 1/2[SP(2) - SP(3)] \\ &\quad - [SCD(2) - SCD(3)] \end{aligned} \quad (8)$$

where $TW(i,j)$ represents the clock difference between ground station i and ground station j , $SP(i)$ represents the time delay of the entire space link when the signal transmitted by ground station i is received by the counterpart station.

III. TRIANGLE CLOSURE EXPERIMENT OF TWSTFT

A. EXPERIMENT PRINCIPLE

An experiment is performed for three ground stations that are distinguished by code division multiple access. Let $TS(n)$ denote the local time scale of station n ; then, the observation

data of stations 1 and 2 can be used to directly calculate the clock difference $[TS(1) - TS(2)]$ between the stations. The clock difference $[TS(1) - TS(3)]$ between ground stations 1 and 3 can similarly be directly calculated from the observation data of stations 1 and 3. The clock difference $[TS(2) - TS(3)]$ between stations 2 and 3 can be indirectly calculated from the actual measured $[TS(1) - TS(2)]$ and $[TS(1) - TS(3)]$ that were directly calculated: $[TS(2) - TS(3)] = [TS(1) - TS(3)] - [TS(1) - TS(2)]$. The clock difference $[TS(2) - TS(3)]$ between ground stations 2 and 3 can also be directly calculated from the observation data for stations 2 and 3. The difference between the direct and indirect clock differences between stations 2 and 3 is the TWSTFT triangle closure difference δ .

The formula is as follows:

$$\delta = TW(2, 3) - [TW(1, 3) - TW(1, 2)] \quad (9)$$

For GEO satellite-based TWSTFT measurements, the space propagation delays of the signals from two ground stations are approximately symmetrical, that is, $SP(i) = SP(j)$, where i and j represent the codes of different ground stations. The Sagnac effect between two-way links based on GEO satellites is approximately constant and can cancel out. Thus, equations (6), (7) and (8) can be simplified and substituted into equation (9) to yield equation (10) given below.

$$\delta = \frac{1}{2} \times \left\{ \left\{ \begin{aligned} & [TI(2) - TI(3)] + [TX(2) - RX(2)] \\ & - [TX(3) - RX(3)] \end{aligned} \right\} - \left\{ \begin{aligned} & [TI(1) - TI(3)] + [TX(1) - RX(1)] \\ & - [TX(3) - RX(3)] \end{aligned} \right\} \right\} - \left\{ \begin{aligned} & [TI(1) - TI(2)] + [TX(1) - RX(1)] \\ & - [TX(2) - RX(2)] \end{aligned} \right\} \right\} \quad (10)$$

TABLE 1. System working status during the performance evaluation test.

Assessment Method	Starting and Ending Time	Ground Station	Links to be Compared	Sampling Interval
TWSTFT triangle closure difference	2020/6/6-2020/6/9	Xi'an	Xi'an-Kashi	The TWSTFT test has one data point per second; 30 minutes is an observation period. In the first 5 minutes of each cycle, the device delay is measured through the satellite simulator.
		Kashi	Xi'an-Sanya	
		Sanya	Kashi-Sanya	
Difference between TWSTFT and PPP				PPP time transfer test has a sample point every 30 seconds; the data of the first 2 hours is used for convergence;

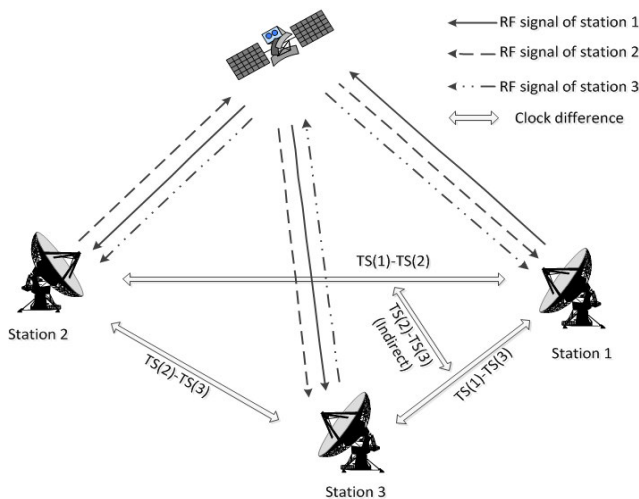


FIGURE 3. System schematic of the triangle closure experiment.

Equation (10) shows that most of the errors in the signal transmission process during the triangle closure experiment cancel out. The value of δ should ideally be zero but is nonzero in practice because of various measurement errors. When ground station 1 receives signals from ground stations 2 and 3, the receiving delays differ among the modem receiving channels, that is, $RX(1,2) \neq RX(1,3)$. Consequently, equation (10) is modified as given below.

$$\delta = \frac{1}{2} \times \left\{ \begin{array}{l} \left\{ \begin{array}{l} [TI(2) - TI(3)] + [TX(2) - RX(2, 3)] \\ - [TX(3) - RX(3, 2)] \end{array} \right\} - \\ \left\{ \begin{array}{l} [TI(1) - TI(3)] + [TX(1) - RX(1, 3)] \\ - [TX(3) - RX(3, 1)] \end{array} \right\} - \\ \left\{ \begin{array}{l} [TI(1) - TI(2)] + [TX(1) - RX(1, 2)] \\ - [TX(2) - RX(2, 1)] \end{array} \right\} \end{array} \right\} \quad (11)$$

where: $RX(i,j)$ represents the reception delay of the equipment when the ground station i receives the signal transmitted by the ground station j .

B. CALIBRATION OF EQUIPMENT DELAY

The calibration principle of the equipment delay at the ground station is shown in Fig. 4. Each ground station uses the time and frequency signals generated by the local atomic clock as external references and inputs these signals to the modem, the up-and-down converter (U/C, D/C), and the

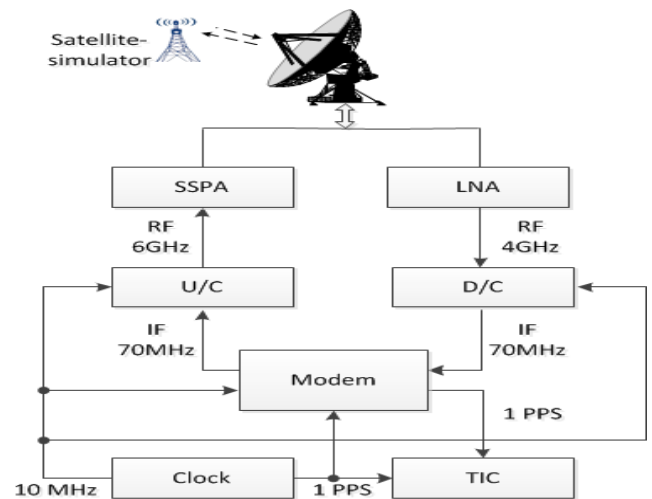


FIGURE 4. Schematic diagram of equipment delay calibration at the ground station. (RF = radio frequency).

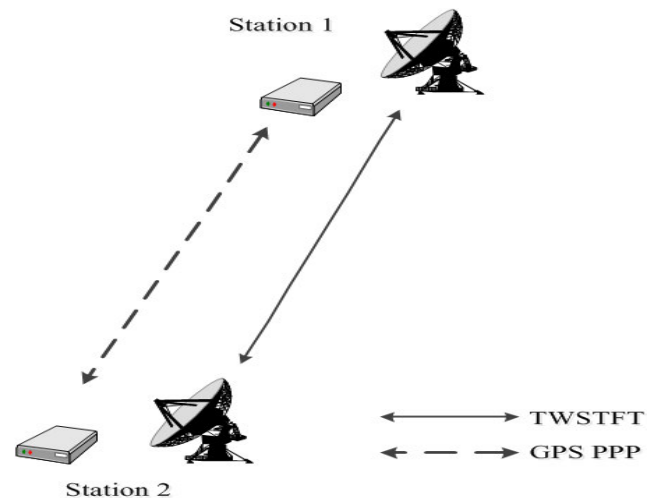


FIGURE 5. Schematic diagram of comparison between TWSTFT and PPP results.

TIC. The modem generates a pseudorandom noise code and outputs a 70-MHz intermediate frequency (IF) signal, which is upconverted to 6 GHz and transmitted by the antenna through an solid-state power amplifier (SSPA). The down-link signal is converted to 4 GHz by the satellite simulator and is received by the parabolic antenna. The signal is

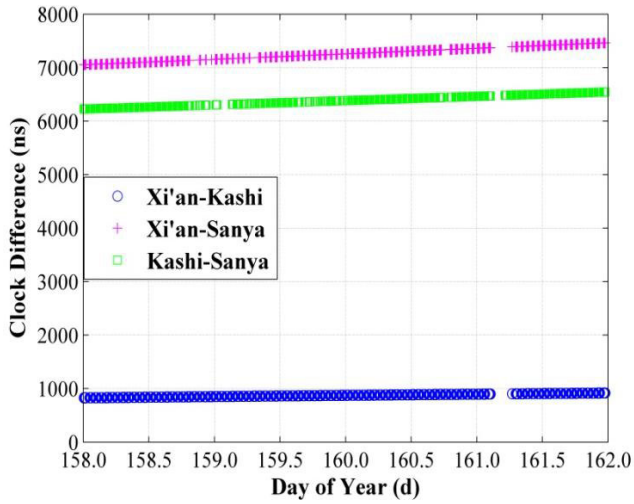


FIGURE 6. Two-way comparison results of Xi'an-Kashi link, Xi'an-Sanya link and Kashi-Sanya link without error correction from June 6 to 9, 2020, UTC time. Among them, Xi'an-Kashi link: peak-to-peak value = 92.1180 ns, Xi'an-Sanya link: peak-to-peak value = 408.3200 ns, Kashi-Sanya link: peak-to-peak value = 316.9290 ns.

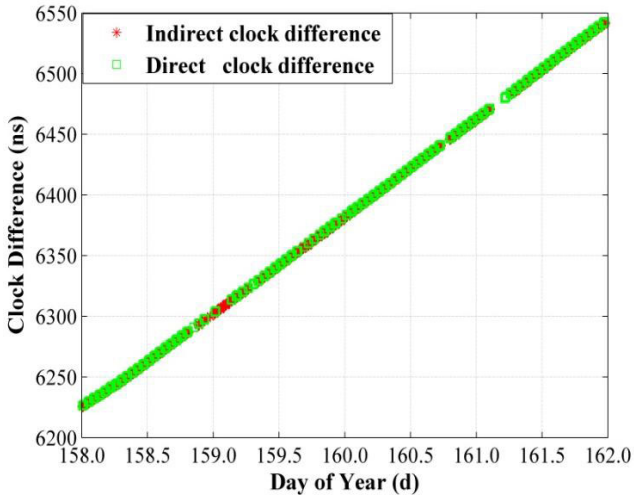


FIGURE 7. Comparison of the direct clock difference and the indirect clock difference of the Kashi-Sanya link from June 6 to 9, 2020 UTC time.

amplified by a low-noise amplifier (LNA), downconverted to an IF of 70-MHz, and sent to a modem for demodulation, whereby the equipment delay of the ground station is obtained.

The equipment delay is a major error that affects the results of the two-way comparison [27]. Implementing TWSTFT for multiple ground stations results in a delay difference between different channels of the multichannel modem, which introduces new errors into the two-way comparison results. The satellite simulator method is used to calibrate the equipment delay with an accuracy of less than 0.5 ns.

We evaluate the accuracy of the triangular closure difference by calculating the root mean square (RMS) value of δ . Detailed calculation method is as following:

$$\delta_{rms} = \left(\frac{1}{N} \sum_{i=1}^N |x_i|^2 \right)^{1/2} \quad (12)$$

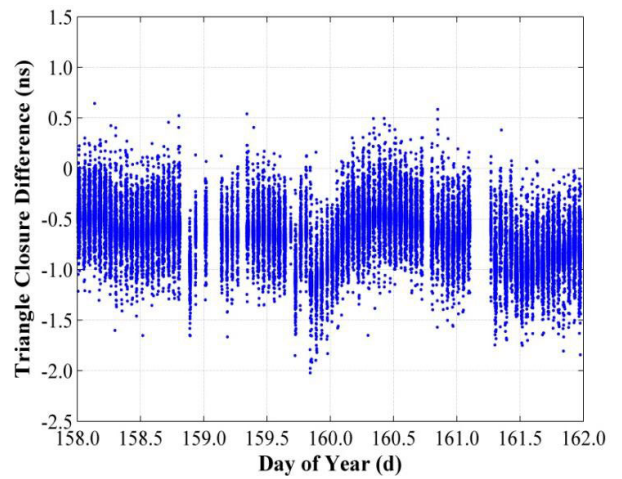


FIGURE 8. The result of triangular closure difference before deducting equipment delay from June 6 to 9, 2020, UTC time. The RMS value is 0.7085 ns.

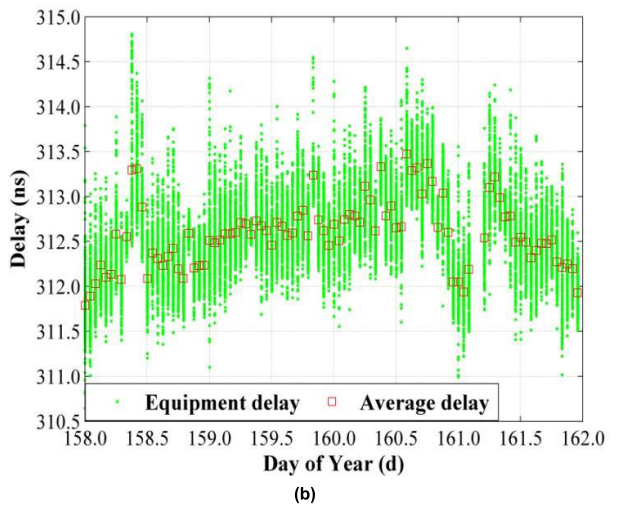
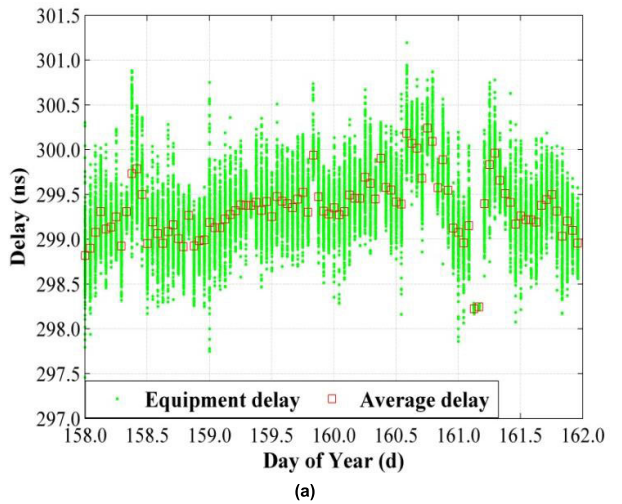


FIGURE 9. From June 6 to 9, 2020, UTC time, the equipment delay measured by different receiving channels of modem in Kashi station. (a) Rx1: peak-to-peak value = 3.7360; (b) Rx2: peak-to-peak value = 4.1620.

in which i stands for time points corresponding to each data point, x_i represents the result of the triangle closure difference at time i , and N stands for sampling numbers.

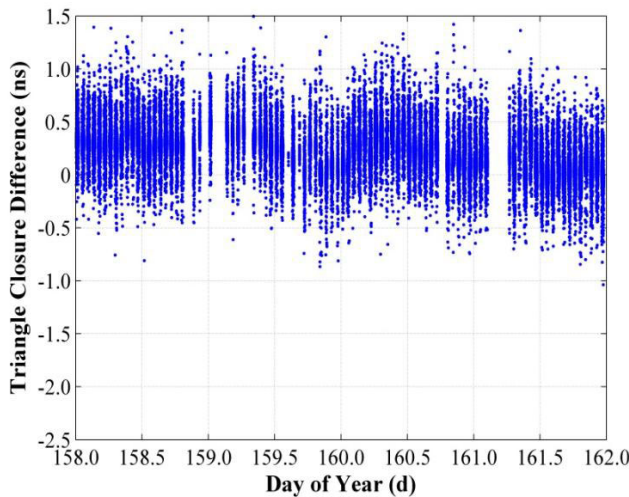


FIGURE 10. The result of triangular closure difference after deducting equipment delay from June 6 to 9, 2020, UTC time. The RMS value is 0.2859 ns.

IV. MUTUAL DIFFERENCE BETWEEN TWSTFT AND PPP TIME TRANSFER

The accuracy of the time transfer between ground stations is further evaluated by carrying out a PPP time transfer test between ground stations during the TWSTFT test. We install an omnidirectional antenna and a global navigation satellite system receiver side-by-side with the parabolic antenna on the ground station to carry out the PPP time transfer experiment. A Trimble NetR9 receiver is used that is connected to the same 10-MHz frequency standard used for the TWSTFT

triangle closure experiment. The accuracy of the time synchronization between ground stations is verified using the mutual difference between the TWSTFT and PPP time transfer, with the GPS PPP time transfer result as an external reference. The verification principle is shown in Fig. 5.

We evaluate the performance by calculating the standard deviation (STD) of the mutual difference results of the TW clock difference and the PPP clock difference. Detailed calculation method is as following:

$$\sigma_{std} = \left(\frac{1}{N-1} \sum_{i=1}^N (x_i - \bar{x})^2 \right)^{1/2} \quad (13)$$

in which i stands for time points corresponding to each data point, x_i represents the mutual difference between TW clock difference and PPP clock difference at time i , \bar{x} represents the average value of the difference between the two clock curves, and N stands for sampling numbers.

V. DATA ANALYSIS AND DISCUSSION

A. EXPERIMENT DETAILS

In this experiment, three ground stations of NTSC were selected, mainly to verify the feasibility of the time transfer performance evaluation method between ground stations proposed in this article. The specific working status during the test is shown in Table. 1.

B. RESULTS OF TWSTFT TRIANGLE CLOSURE DIFFERENCE

The data processing results of the TWSTFT triangle closure difference are shown in Figs. 6 to 10. Fig. 7 compares the

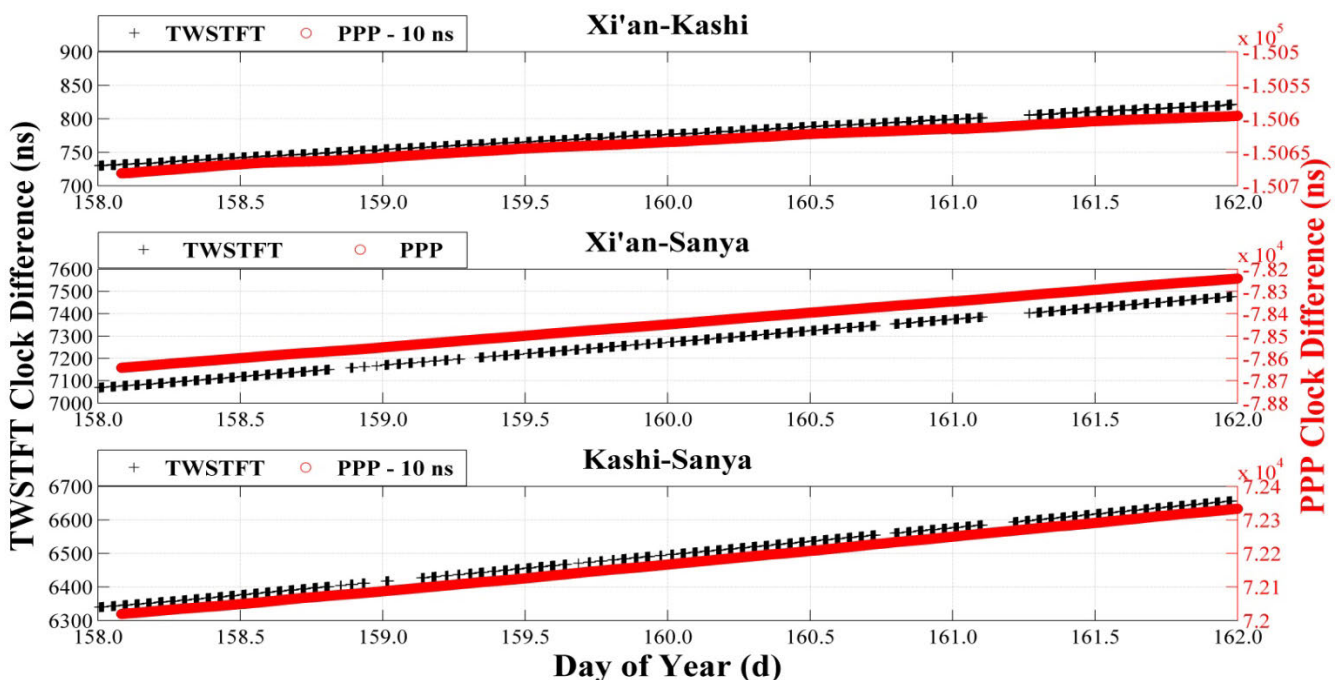


FIGURE 11. UTC time June 6-9, 2020, the three comparison links used TWSTFT and PPP technology to obtain the time comparison results between stations. Among them, for the Xi'an-Kashi link, the peak-to-peak value of the TWSTFT curve is 92.1110ns, and the peak-to-peak value of the PPP curve is 86.0977 ns; for the Xi'an-Sanya link, the peak-to-peak value of the TWSTFT curve is 408.3170 ns, and the peak-to-peak value of the PPP curve is 400.0459 ns; for the Kashi-Sanya link, the peak-to-peak value of the TWSTFT curve is 316.9310 ns, and the peak-to-peak value of the PPP curve is 314.0257 ns.

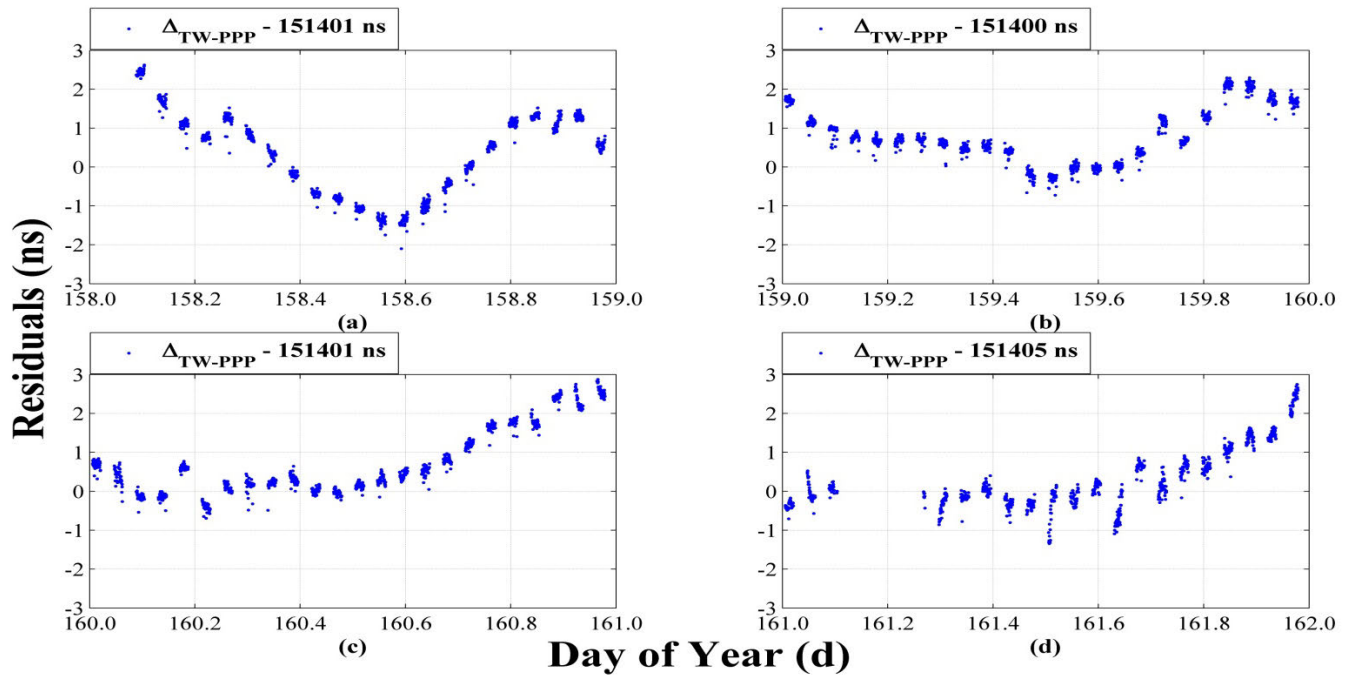


FIGURE 12. For June 6-9, 2020, UTC time, the result of the mutual difference between the TW clock difference and the PPP clock difference of the Xi'an-Kashi comparison link. (a) STD=1.053 ns; (b) STD=0.693 ns; (c) STD=0.866 ns; (d) STD=0.780 ns.

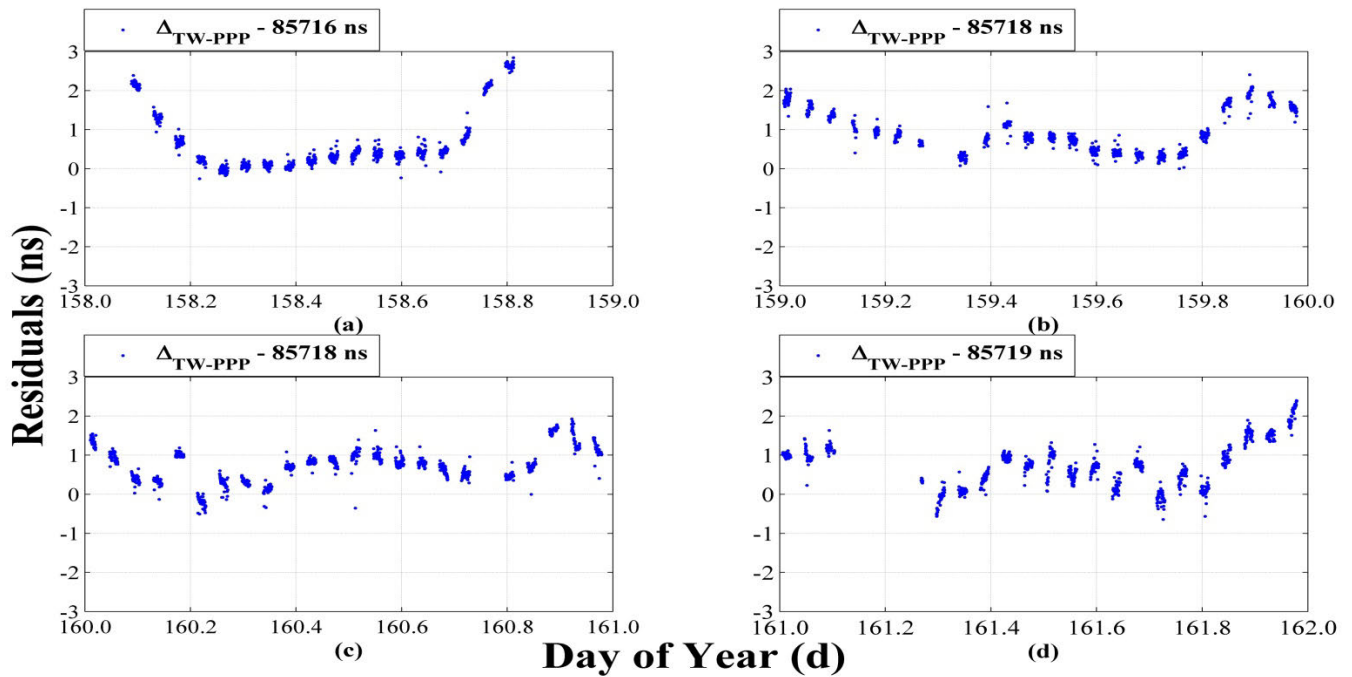


FIGURE 13. For June 6-9, 2020, UTC time, the result of the mutual difference between the TW clock difference and the PPP clock difference of the Xi'an-Sanya comparison link. (a) STD=0.980 ns; (b) STD=0.530 ns; (c) STD=0.440 ns; (d) STD=0.578 ns.

direct and indirect clock differences for the Kashi-Sanya comparison link. Fig. 8 shows the difference between the direct and indirect clock differences for the Kashi-Sanya comparison link, that is, the triangle closure difference. We use the satellite simulator method as an independent measure of the device delays of the different receiving channels of the multichannel modem. Fig. 9 shows the equipment delay measured by different receiving channels of the same modem

at Kashi Station. Fig. 10 shows the triangle closure result obtained after deducting the respective equipment delays of the three ground stations. Comparing Figs. 8 and 10 shows that the equipment delay is the error with the largest impact on the closure difference for the GEO-satellite-based TWSTFT triangular closure test. Deducting the equipment delay from the TWSTFT triangle closure difference produces a RMS value of less than 0.3 ns.

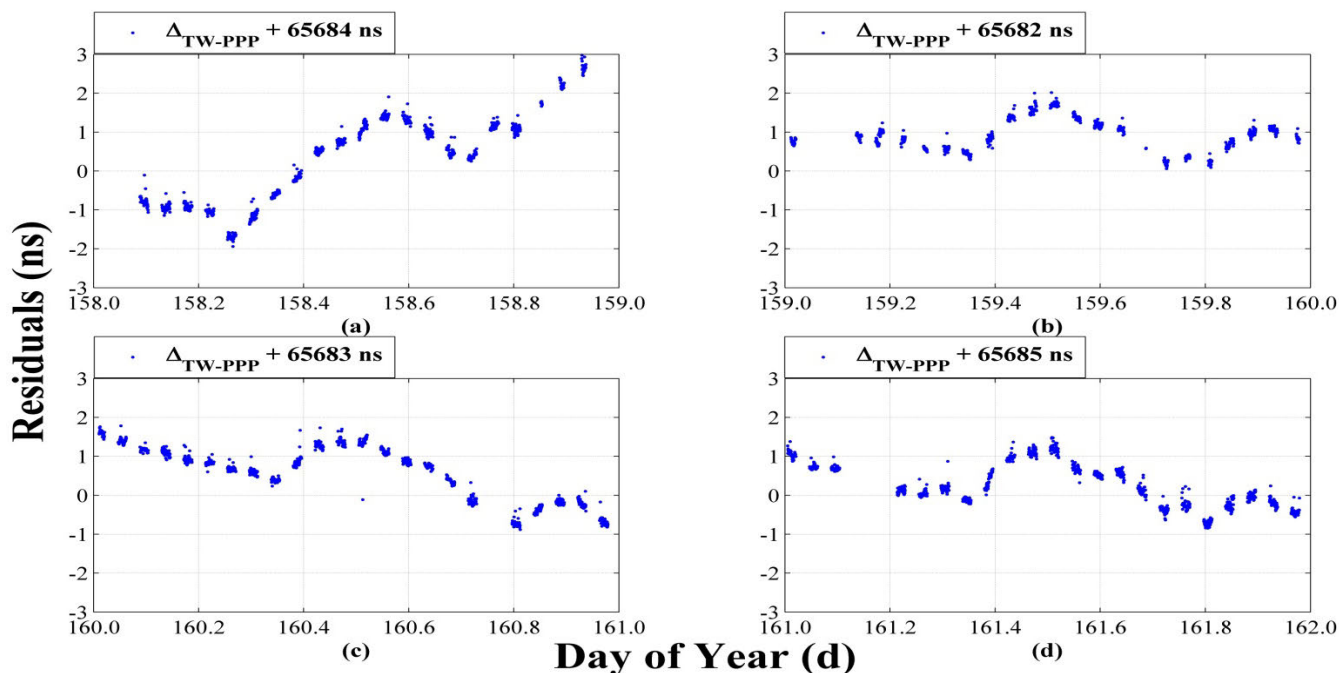


FIGURE 14. For June 6-9, 2020, UTC time, the result of the mutual difference between the TW clock difference and the PPP clock difference of the Kashi-Sanya comparison link. (a) STD=1.112 ns; (b) STD=0.418 ns; (c) STD=0.684 ns; (d) STD=0.546 ns.

TABLE 2. Statistics of the mutual difference results of the daily TW clock difference and PPP clock difference of the three comparison links. (unit: ns).

Links to be Compared	2020.06.06	2020.06.07	2020.06.08	2020.06.09	AVG ₆₋₉	AVG ₇₋₉
Xi'an-Kashi	1.053	0.693	0.866	0.780	0.848	0.780
Xi'an-Sanya	0.980	0.530	0.440	0.578	0.632	0.516
Kashi-Sanya	1.112	0.418	0.684	0.546	0.690	0.550

note: AVG₆₋₉ represents the average of STD results from June 6th to 9th. AVG₇₋₉ represents the average of STD results from June 7th to 9th.

C. MUTUAL DIFFERENCE RESULT BETWEEN TWSTFT AND PPP TIME TRANSFER

The data processing results of the difference between TWSTFT and PPP are shown in Figs. 11 to 14 respectively. Among them, Fig. 11 shows the time comparison results of three comparison links based on TWSTFT and PPP technology. The results for the Xi'an-Kashi and Kashi-Sanya links shown in Fig. 11 are not easily observable because of the overlap between the two clock difference curves; thus, the PPP clock differences for the two compared links are reduced by 10 ns. Fig. 11 shows clear deviations between the clock difference results because of systematic error between the two sets of different devices. As the same time-frequency reference is used, the same general trends are observed for the two clock difference curves and the drift of the clock over 4 days. Figs. 12 to 14 show the daily STD results of the three comparison links from June 6th to June 9th. To facilitate observation, we subtract the integer part of the average value of the mutual difference results for each curve during data processing.

For the convenience of comparison, we organize the results in Fig. 12 to Fig. 14 in Table. 2. By calculating the daily STD of the three comparison links from June 6th to June 9th,

it is found that the STD result on June 6th is significantly larger than the other three days. After our analysis, we believe that this may be caused by the maneuver of the APSTAR-7 satellite on the day of the experiment. After excluding the data on June 6, the mutual difference results of the daily TW clock difference and PPP clock difference of the three comparison links are in good agreement.

VI. CONCLUSION

The objective of this study is the facile and rapid performance evaluation of an NTSC two-way satellite comparison network without the use of additional equipment, which is achieved by applying the TWSTFT triangle closure method and the PPP time transfer method to the network. The time transfer performance of the network is thus determined. The two evaluation methods have been presented in detail, and the Xi'an, Kashi and Sanya stations of the NTSC two-way satellite comparison network are selected to carry out verification experiments. The results show that the equipment delay of the ground station has a significant effect on the triangle closure difference. Subtracting the channel delay from the triangle closure difference yields a value below 0.3 ns. Moreover, the mutual difference between the TWSTFT and

PPP time transfer experiments results is less than 0.6 ns, which is consistent with the TWSTFT accuracy. Thus, it is feasible to apply the proposed evaluation method to the NTSC two-way satellite comparison network. Redundant links are used to evaluate the performance of the two-way satellite comparison network without the use of additional equipment. This method is also applicable to terrestrial systems with similar networks and can be used to expand the application of TWSTFT technology.

REFERENCES

- [1] Z. Jiang, "Towards a TWSTFT network time transfer," *Metrologia*, vol. 45, no. 6, pp. S6–S11, Dec. 2008.
- [2] H.-T. Lin, Y.-J. Huang, W.-H. Tseng, C.-S. Liao, and F.-D. Chu, "Recent development and utilization of two-way satellite time and frequency transfer," *MAPAN*, vol. 27, no. 1, pp. 13–22, Mar. 2012.
- [3] Y.-J. Huang, H.-W. Tsao, H.-T. Lin, and C.-S. Liao, "Multiple access interference suppression for TWSTFT applications," *IEEE Trans. Instrum. Meas.*, vol. 66, no. 6, pp. 1337–1342, Jun. 2017.
- [4] K. Verhasselt and P. Defraigne, "Multi-GNSS time transfer based on the CGGTTS," *Metrologia*, vol. 56, no. 6, pp. 1–12, Oct. 2019.
- [5] S. L. Wang, X. W. Zhao, Y. L. Ge, and X. H. Yang, "Investigation of real-time carrier phase time transfer using current multi-constellations," *Measurement*, vol. 166, pp. 1–11, Jul. 2020.
- [6] D. Kirchner, "Two-way satellite time and frequency transfer (TWSTFT): Principle, implementation, and current performance," in *Review of Radio Science*. New York, NY, USA: Oxford Univ. Press, 1999, pp. 27–44.
- [7] X. H. Yang, Z. G. Li, and A. H. Hua, "Analysis of two-way satellite time and frequency transfer with C-band," in *Proc. IFCS*, Geneva, Switzerland, 2007, pp. 901–903.
- [8] N. Guyennon, G. Cerretto, P. Tavella, and F. Lahaye, "Further characterization of the time transfer capabilities of precise point positioning (PPP)," in *Proc. IFCS*, Geneva, Switzerland, May 2007, pp. 399–404.
- [9] D. Orgiazzi, P. Tavella, and F. Lahaye, "Experimental assessment of the time transfer capability of precise point positioning (PPP)," in *Proc. IFCS*, Vancouver, BC, Canada, Aug. 2005, pp. 29–31.
- [10] F. Arias, Z. Jiang, W. Lewandowski, and G. Petit, "BIPM comparison of time transfer techniques," in *Proc. FCSE*, Vancouver, BC, Canada, 2005, pp. 312–315.
- [11] G. Petit and Z. Jiang, "Precise point positioning for TAI computation," *Int. J. Navigat. Observ.*, vol. 2008, pp. 1–8, Feb. 2008.
- [12] Z. Jiang and G. Petit, "Combination of TWSTFT and GNSS for accurate UTC time transfer," *Metrologia*, vol. 46, no. 3, pp. 305–314, Apr. 2009.
- [13] Z. Li, X. Yang, G. Ai, H. Si, R. Qiao, and C. Feng, "A new method for determination of satellite orbits by transfer," *Sci. China G, Phys., Mech. Astron.*, vol. 52, no. 3, pp. 384–392, Mar. 2009.
- [14] C. Fen, Y. Xuhai, S. Mudan, L. Zhigang, C. Liang, L. Weichao, S. Baoqi, K. Yao, W. Pei, and F. Chugang, "Evaluation of C-band precise orbit determination of geostationary Earth orbit satellites based on the Chinese area positioning system," *J. Navigat.*, vol. 67, no. 2, pp. 343–351, Mar. 2014.
- [15] W. Wang, X. Yang, S. Ding, W. Li, H. Su, P. Wei, F. Cao, L. Chen, J. Gong, and Z.-G. Li, "An improved protocol for performing two-way satellite time and frequency transfer using a satellite in an inclined geo-synchronous orbit," *IEEE Trans. Ultrason., Ferroelectr., Freq. Control*, vol. 65, no. 8, pp. 1475–1486, Aug. 2018.
- [16] Z. Jiang, S. Y. Lin, and W. H. Tseng, "Fully and optimally use the redundancy in a TWSTFT network for accurate time transfer," in *Proc. EFTF/IFCS*, Besancon, France, Jul. 2017, pp. 676–680.
- [17] V. Zhang, T. Parker, and S. Zhang, "A study on Reducing the Diurnal in the Europe-to-Europe TWSTFT Links," in *Proc. EFTF*, York, U.K., Apr. 2016, pp. 1–4.
- [18] D. Matsakis, L. Breakiron, A. Bauch, D. Piester, and Z. Jiang, "Two-way satellite time and frequency transfer (TWSTFT) calibration constancy from closure sums," in *Proc. PTIT*, Reston, VA, USA, Dec. 2008, pp. 587–604.
- [19] Z. Jiang, W. Lewandowski, and D. Piester, "Calibration of TWSTFT links through the triangle closure condition," in *Proc. PTIT*, Reston, VA, USA, Dec. 2008, pp. 467–484.
- [20] Z. Jiang, D. Matsakis, V. Zhang, H. Esteban, D. Piester, S. Y. Lin, and E. Dierikx, "A TWSTFT calibration guideline and the use of a GPS calibrator for UTC TWSTFT link calibrations," in *Proc. PTIT*, Monterey, CA, USA, Jan. 2016, pp. 231–242.
- [21] Z. Jiang, D. Piester, C. Schlunegger, E. Dierikx, V. Zhang, J. Galindo, and D. Matsakis, "The 2015 TWSTFT calibration for UTC and related time links," in *Proc. EFTF*, York, U.K., Apr. 2016, pp. 1–4.
- [22] M. C. Martínez-Belda and P. Defraigne, "Combination of TWSTFT and GPS data for time transfer," *Metrologia*, vol. 47, no. 3, pp. 305–316, Apr. 2010.
- [23] P. Defraigne, M. C. Martínez, and Z. Jiang, "Time transfer from combined analysis of GPS and TWSTFT data," in *Proc. PTIT*, Reston, VA, USA, Dec. 2008, pp. 565–576.
- [24] *The Operational Use of Two-Way Satellite Time and Frequency Transfer Employing Pseudorandom Noise Codes*, document ITU-R TF.1153-4, ITU Radiocommunication Sector, Geneva, Switzerland, Aug. 2015. [Online]. Available: <http://www.itu.int/rec/R-REC-TF.1153-4-201508-I/en>
- [25] W.-H. Tseng, K.-M. Feng, S.-Y. Lin, H.-T. Lin, Y.-J. Huang, and C.-S. Liao, "Sagnac effect and diurnal correction on two-way satellite time transfer," *IEEE Trans. Instrum. Meas.*, vol. 60, no. 7, pp. 2298–2303, Jul. 2011.
- [26] T. E. Parker and V. Zhang, "Source of instabilities in two-way satellite time transfer," in *Proc. FCSE*, Vancouver, BC, Canada, 2005, pp. 745–751.
- [27] T. T. Thai, I. Sesia, G. D. Rovera, and J. Achkar, "Characterization of delays for spare SATRE modems in TWSTFT stations," in *Proc. EFTF/IFCS*, Orlando, FL, USA, Apr. 2019, pp. 1–3.



WEI WANG received the B.S. degree in electronic information engineering from Yan'an University, Yan'an, Shaanxi, China, in 2013, and the Ph.D. degree in astrometry and celestial mechanics from the University of Chinese Academy of Sciences, Beijing, China, in 2020.

Since 2020, he has been an Engineer with the Department of Orbit and Time Transfer, National Time Service Centre, Chinese Academy of Science. His research interests include orbit measurement, orbit determination, and time transfer.



XUHAI YANG was born in Weinan, Shaanxi, China, in 1972. He received the B.S. degree in applied physics from the Northeastern University, Shenyang, in 1995, and the Ph.D. degree in astrometry and celestial mechanics from the Graduate School, Chinese Academy of Sciences, Beijing, in 2003.

Since 2007, he has been serving as the Director of the Department of Research on high-precision time transfer and precision orbit determination.

He has authored two books, more than 30 articles, and several patents. His research interests include high-precision time transfer, orbit measurement, and orbit determination.



WEICHAO LI was born in Xi'an, Shaanxi, China, in 1980. He received the B.S. and M.S. degrees from Northwestern Polytechnical University, Xi'an, China, in 2002 and 2005, respectively, and the Ph.D. degree from the Graduate University, Chinese Academy of Sciences, Beijing, China, in 2009.

Since 2005, he has been a Faculty Member with the National Time Service Center, Chinese Academy of Sciences. He has been in charge of and joined more than ten science projects. He has authored or coauthored more than 20 academic articles. His research interests include satellite orbit tracking and determination, high precise remote time transfer, and equipment calibration of time delay.



YULONG GE received the Ph.D. degree from the National Time Service Center, University of Chinese Academy of Sciences, in 2020. His current research mainly focuses on multi-constellation and multi-frequency GNSS time transfer timing and positioning.



PEI WEI received the B.S. degree in computer science from Northwest Polytechnic University, Xi'an, China, in 2010, and the M.S. degree in measuring and testing technologies and instruments and the Ph.D. degree in astrometry and celestial mechanics from the University of Chinese Academy of Sciences, Beijing, China, in 2013 and 2020, respectively.

Since 2013, he has been a Research Associate with the Department of Orbit and Time Transfer, National Time Service Center, Chinese Academy of Sciences. His research interests include orbit measurement, orbit determination, and time transfer.



LIANG CHEN was born in Weinan, Shaanxi, China, in 1976. He received the B.S. degree in computational engineering from the University of Electronic Science and Technology of China, Chengdu, in 1998, and the M.S. degree in measuring and testing technologies and instruments from the Graduate School, Chinese Academy of Sciences, Beijing, China, in 2010.

Since 2010, he has been a Faculty Member with the National Time Service Center, Chinese Academy of Sciences. His research interests include high-precision time transfer, and orbit measurement and determination.



PENG LIU received B.S. and M.S. degrees in control science and engineering from Taiyuan University of Technology, in 2010 and 2013, respectively.

Since 2013, he has been an Engineer with the 39th Research Institute, China Electronics Technology Group Corporation. His research interests are satellite communication and servo drive.



FEN CAO was born in Jinan, Shandong, China, in 1985. She received the B.S. degree in the communication engineering from Shandong Normal University, Jinan, China, in 2008, and the M.S. degree in communication and information system and the Ph.D. degree in astrometry and celestial mechanics from the University of Chinese Academy of Sciences, Beijing, China, in 2011 and 2014, respectively.

Since 2014, she has been a Faculty Member with the National Time Service Center, Chinese Academy of Sciences. Her research interest is satellite precision orbit determination.



ZHIGANG LI received the B.S. degree in astronomy from Nanjing University, Nanjing, China, in 1966.

Since 1968, he has been engaged in scientific research with the Shaanxi Astronomical Observatory, Chinese Academy of Sciences, and a Ph.D. Supervisor. He served as the Director of the Research Office and the Academic Committee of the National Time Service Center. His research interests include high-precision time transfer, orbit measurement, and orbit determination.

...